Temperature Compensation Model for Monitoring Sensor in Steel Industry Load Management

Liyuan Sun[1], Zeming Yang[2,5*], Nan Pan[3], Shilong Chen[4], Yaoshen He[3,5], Junwei Yang[5]

[1]Measurement Center, Yunnan Power Grid Co., Ltd., Kunming, China

[2]Faculty of Civil Aviation and Aeronautical, Kunming University of Science & Technology, Kunming, China

[3]Faculty of Transportation Engineering, Kunming University of Science & Technology, Kunming, China

[4]Yuxi Power Supply Bureau, Yunnan Power Grid Co., Ltd., Yuxi, China,

[5]LongShine Technology Group Co., Ltd., Wuxi, China

Received 23 April 2024; received in revised form 03 July 2024; accepted 04 July 2024

DOI: https://doi.org/10.46604/ijeti.2024.13621

Abstract

The iron ore industry faces increasing electricity demand due to industrialization, making effective management of electricity demand crucial. This study proposes a temperature compensation model using Support Vector Regression (SVR), aiming to enhance the accuracy of sensors in monitoring electricity demand. An experiment is conducted to assess the impact of temperature on sensor measurements, and a modified Whale Optimization Algorithm is employed to correct the sensor outputs. The proposed model is compared with both PSO-SVR and unimproved WOA-SVR. Results show that the proposed model significantly improves accuracy, achieving a determination coefficient of 0.7882 and a relative standard deviation of the error square sum of 4.6412%. The results of this study not only enhance power demand management in iron mining but also hold potential applications across various industries.

Keywords: power systems, temperature compensation, SVR, improved whale optimization algorithm

1. Introduction

In recent years, amidst the rapid evolution of the global economy and the swift pace of industrialization, energy demand has emerged as a pivotal factor constraining the sustainable development of nations [1-4]. The iron ore power industry stands as a cornerstone of national economic and social progress [5-8]. Nonetheless, challenges persist in managing demand effectively within the iron ore power sector. At the heart of these challenges lies the issue of how temperature fluctuations impact the performance of monitoring sensors. These sensors play a pivotal role in the iron ore power system, facilitating real-time monitoring of operational status, temperature, and other critical parameters of power equipment. However, the variability in ambient temperature can lead to deviations in sensor performance, thereby compromising the accuracy of monitoring and management within the power system. Thus, enhancing measurement precision necessitates the implementation of temperature compensation mechanisms for the sensors [9].

Currently, temperature compensation methods commonly employed are categorized into hardware compensation and software compensation [10]. Hardware compensation relies on exploiting the inverse temperature coefficient of an additional component to counteract the temperature drift coefficient inherent in the sensor, offering the advantages of simplicity and real-

* Corresponding author. E-mail address: yangzeming@stu.kust.edu.cn

English language proofreader: Yen-Chun Hsieh

time response. For instance, Sheng et al. [11] introduced a high-precision, cost-effective compensation technique along with a novel internal compensation mechanism aimed at mitigating the significant impact of temperature drift on the measurement accuracy of fiber Bragg grating (FBG) sensors caused by Fabry-Perot (F-P) filter. Employing least squares support vector regression (LSSVR), a temperature drift model is established, effectively addressing issues of substantial errors and sluggish computation.

Gan et al. [12] developed a dual-axis sensor with a temperature compensation function based on fiber grating for vascular interventional surgery. Its four FBG-embedded fibers are suspended in a circular array inside the flexure hinge to minimize transverse strain crosstalk and improve measurement accuracy. The temperature compensation effect of the sensor can be used for accurate force measurement under different temperature conditions. Meanwhile, Zhang et al. [13] outlined the design principles of an on-chip temperature compensation interface ASIC, leveraging the amplitude of the drive feedback AC voltage signal as a virtual temperature sensor. This innovative approach enables on-chip temperature compensation for gyroscope output angular velocity signals, enhancing overall system performance and reliability.

To address the issue of low sensitivity or limited detection range encountered with SPR sensors, Tian et al. [14] have introduced a cascaded fiber SPR sensor boasting high sensitivity along with a temperature compensation feature. This innovation offers the potential for highly efficient and accurate detection even in complex environmental conditions. Nevertheless, the existing hardware compensation methods commonly employed suffer from drawbacks such as limited accuracy, cumbersome calibration processes, and increased expenses, thus hindering their practical viability in engineering applications [10].

Software compensation involves acquiring data through calibration experiments and using algorithms or models to establish a mapping relationship between sensor input and output. In contrast to hardware compensation, software compensation offers the advantages of high precision and low cost. For instance, Wang et al. [15] proposed an INS temperature drift compensation method based on gravitational search algorithm (GSA) tuned support vector regression (SVR) to solve the problem that the traditional temperature drift compensation method requires a long time to calibrate each inertial sensor separately. This method has better performance and significantly improves compensation accuracy and efficiency.

To solve the influence of temperature on the gyroscope, Ouyang et al. [16] established a temperature compensation model for the output signal of the gyroscope by using Long Short-Term Memory (LSTM), Support Vector Machine (SVM) and Deep Belief Network (DBN). A denoising algorithm using Variational Mode Decomposition (VMD) and Sampling Entropy (SE) was developed to eliminate the influence of factors other than temperature on the MEMS gyroscope. Finally, temperature experiments show that the rate of random drift and bias instability of the gyroscope compensation output signal is significantly reduced. Aiming at the problem that the accuracy of traditional SOC estimation algorithms decreases significantly under low temperature and low SOC conditions, Chen et al. [17] designed a new SOC estimation framework, which combines a new radial basis function neural network (RBFNN) battery model, temperature compensation strategy and unscented Kalman filter (UKF). The experimental results show that the framework has excellent generalization performance.

Yu et al. [18] proposed an unsupervised deep network (DNTC) method to compensate for the temperature of non-stationary data. This method not only effectively deals with large-scale sequences, but also takes into account their non-stationary characteristics, showing excellent compensation effect. Zhao et al. [19] introduced an enhanced surface fitting method leveraging the improved grey wolf algorithm (IGWO), devising a robust mathematical framework for comprehensive compensation to effectively counteract nonlinearities and temperature-induced drift in sensors. To improve the bias stability of fiber optic gyroscope (FOG) inertial navigation systems in different ambient temperature environments, Tian et al. [20] proposed a new temperature compensation method based on the correlation analysis of the same batch of FOGs. Experiment results show that the proposed method has an excellent compensation effect for both high-precision and low-precision FOG.

To improve the ranging accuracy of UWB, Sheng Liu et al. established a temperature compensation model for ranging error by analyzing the influence of temperature and humidity on ranging results. The relationship between timestamp delay error and actual distance was also explored. Finally, a hybrid compensation model based on temperature and distance was obtained. The statistical results show that the hybrid compensation model has strong environmental robustness [21]. In a similar vein, Bobobee et al. [22] propose an improved particle swarm optimization-long short-term memory (IPSO-LSTM) model with temperature compensation ability for SOC estimation of lithium-ion batteries. The model combines the advantages of PSO and LSTM and has better accuracy and robustness [22]. However, the model or algorithm used in software compensation at this stage is highly complex and the compensation accuracy is low.

Therefore, this paper proposes an SVR temperature compensation model based on the improved Whale Optimization Algorithm (WOA) optimization. WOA is used to optimize the penalty factor and kernel function of the SVR model globally, which reduces the influence of hyperparameter selection on the compensation accuracy of the SVR model and improves its effectiveness, to provide more accurate load forecasting for power demand of iron and steel industry.

2. Support Vector Regression Model

Support Vector Regression (SVR) is a Support Vector Machine (SVM) improvement and application. The main difference is that SVR aims to find an optimal hyperplane to minimize the total variance of all sample points relative to the plane. SVR achieves this goal by optimizing the problem, and has the advantages of robustness to outliers, simple decision model update, and high prediction accuracy. As shown in the following figure, Fig.1 represents the Partition line division of sample space; Fig. 2 shows the support vector nonlinear regression structure.

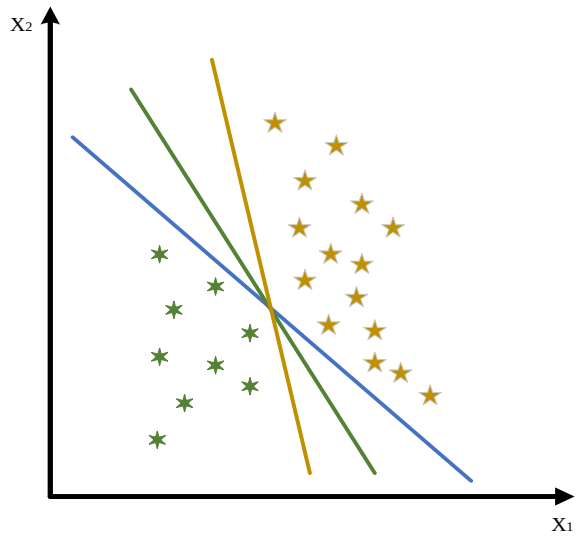

Fig. 1 Partition line division of sample space

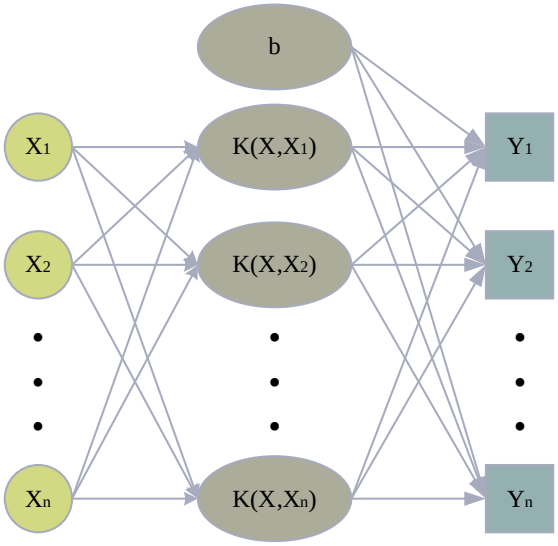

Fig. 2 Support vector nonlinear regression structure

For a given temperature data set $\{(x_1, y_1),(x_2, y_2),\cdots,(x_n, y_n)\}$, the SVR model is trained to represent the relationship between the sensor temperature x and the compensated temperature y by regression function. By assigning to x, the function can get the corresponding predicted value, and the regression function is:

$$f(x) = \omega^T \varphi(x) + b \tag{1}$$

where $f(x)$ is the predicted target value; ω is a weight vector; which is a mapping function of $\varphi(x)$ from low-dimensional space to high-dimensional space concerning x; b is the bias term.

The basic form of SVR is to solve the model parameters by minimizing the loss function. According to the principle of structural risk minimization, it can be concluded that:

$$\min_{\omega,b} Q = \frac{1}{2}\|\omega\| + C\sum_{i=1}^{n}(\xi_i + \xi_i)$$
$$s.t.\begin{cases} y_i - [\omega \cdot \varphi(x_i) + b] \le \varepsilon + \xi_i \\ [\omega \cdot \varphi(x_i) + b] - y_i \le \varepsilon + \xi_i \\ \xi_i, \xi_i \ge 0 \end{cases} \tag{2}$$

In the context of this equation, $\min Q$ represents the minimum value of the objective function. The weight vector is denoted by ω, while C represents the penalty factor. The variables ξ_i and ξ_i are slack variables, enabling some data points to deviate from the hyperplane. Specifically, ξ_i accounts for cases where the predicted value is lower than the actual value, while ξ_i corresponds to instances where the predicted value exceeds the actual value. Additionally, ε represents a predefined tolerance parameter crucial for determining the range of support vectors.

By introducing the Lagrange multiplier $\alpha_i, a_i, \mu_i, \mu_i$, the above optimization problem is transformed into a convex quadratic programming problem. The optimization problem is then converted into a dual problem through the pairing of ω, b, ξ, ξ, resulting in the following equations:

$$\omega = \sum_{i=1}^{n}(\alpha_i - \alpha_i)x_i$$
$$b^* = y_i + \varepsilon - \sum_{i=1}^{n}(\alpha_i^* - a_j^*)x_i^T x_j \tag{3}$$
$$b^* = y_i - \varepsilon - \sum_{i=1}^{n}(\alpha_i^* - a_j^*)x_i^T x_j$$

By introducing a kernel function, the nonlinear data samples are mapped to the high-dimensional data space, and the nonlinear fitting expression for temperature compensation is as follows:

$$f(x) = \sum_{i=1}^{n}\left(\alpha_i^* - \alpha_i^*\right)K(x,y) + b^* \tag{4}$$

Here $K(x, y)$ is a kernel function that can realize nonlinear mapping. Through the kernel function, the problem can be transformed into a linear problem in high-dimensional space, which simplifies the problem. In the temperature compensation model, the kernel function is usually a Gaussian radial basis kernel function (standard deviation is σ), and the expression is:

$$K(x,y) = \exp\left(-\frac{\|x-y\|^2}{2\sigma^2}\right) \tag{5}$$

The SVR flowchart is shown in Fig. 3:

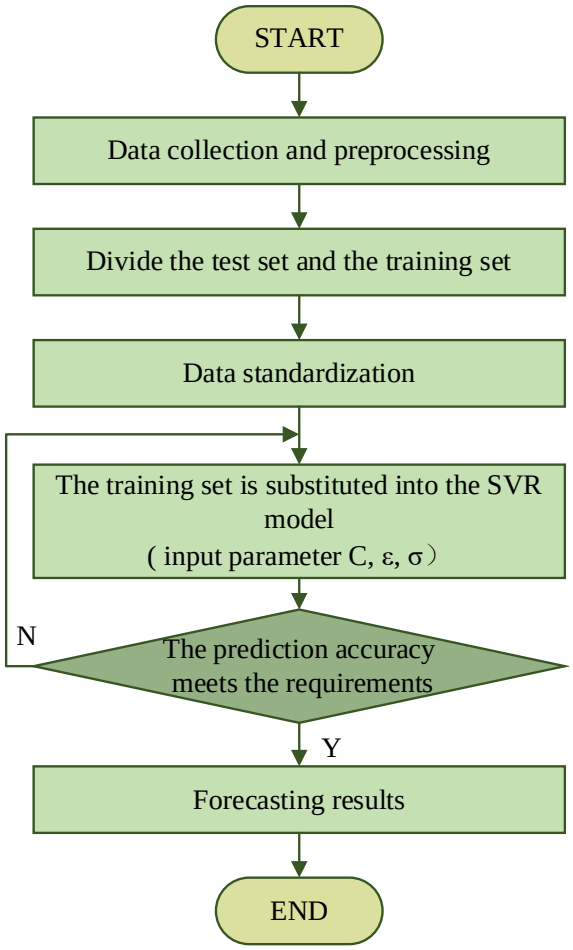

Fig. 3 SVR calculation flow chart

3. Whale Optimization Algorithm and Its Improvement

After obtaining the SVR model, to optimize the parameters such as penalty factor and kernel function in the SVR model efficiently, a highly competitive swarm intelligence optimization algorithm is designed to obtain high-quality multi-dimensional parameters. Given the advantages of the whale optimization algorithm with fewer parameters and excellent global search performance, this paper aims to enhance the whale optimization algorithm to improve the efficiency and effectiveness of the SVR model.

3.1 Whale Optimization Algorithm

The Whale Optimization Algorithm (WOA) is an intelligent optimization algorithm that mimics the hunting behavior of whales. It operates in three key stages: encircling predation, spiral update, and prey search. The WOA harnesses group intelligence to efficiently tackle complex optimization challenges.

(1) Surrounding predation

In the predation stage, the whale group guides the nearest whale individual (i.e., the current optimal solution) to the vicinity of the prey by obtaining the prey location information, to encourage the whole group to gradually approach the prey. In practical problems, the global optimal solution of the problem is equivalent to the location of the prey. The mathematical expression at this stage is:

$$X(t+1) = X^*(t) - A \cdot D \tag{6}$$

$$D = \left| C \cdot X^*(t) - X(t) \right| \tag{7}$$

where t represents the number of iterations; $X(t+1)$ is the position vector of the whale individual; $X^*(t)$ is the position vector of prey; D is the distance between the whale individual and the prey position; both A and C are coefficient vectors, and the specific formula is shown in Equation (8) :

$$\begin{cases} A = 2\alpha \cdot r_1 - \alpha \\ C = 2 \cdot r_2 \\ \alpha(t) = 2 - 2t / T_{\max} \end{cases} \tag{8}$$

In the formula, r_1 and r_2 are random variables in the range [0,1] respectively; α is the coefficient vector related to the number of iterations, composed of $\alpha(t)$; $T_{\max}$ is the maximum number of iterations.

(2) Spiral update

In the process of spiral update, the whale takes the prey as the center gradually approaches the prey through the continuous spiral rise, and finally successfully captures the target. To ensure the synchronization of contraction encirclement and spiral approximation, the position update mode of the whale individual is judged by probability p . Assuming that the probability of both modes is 50 %, the position update formula in this process is expressed as:

$$X(t+1) = \begin{cases} X^*(t) - A \cdot D & p < 0.5 \\ D \cdot e^{bl} \cdot \cos(2\pi l) + X^*(t) & p \geq 0.5 \end{cases} \tag{9}$$

where b is used to define the spiral coil, which is a constant; l is a random number in the range of [-1,1].

(3) Search for prey

In the prey search phase, whale individuals find new potential solutions through a random search, so individuals are randomly selected from the population for location updates. The expression of this phase is as follows:

$$X(t+1) = X_r(t) - A \cdot D \tag{10}$$

$$D = \left| C \cdot X_r(t) - X(t) \right| \tag{11}$$

$X_r(t)$ in the formula represents the position vector of whale individuals randomly selected in the current population. When the coefficient $|A| \geq 1$, the whale is outside the shrinking enclosure, and a random search is performed at this time; when $|A| < 1$, the whale is in the enclosure, select the spiral surround search.

3.2 Improved Whale Optimization Algorithm

The paper refines the Whale Optimization Algorithm by integrating chaotic mapping for initial population diversity and an adaptive weight mechanism to balance search exploration and exploitation, thereby improving convergence speed and overall performance.

(1) Initial population based on chaos mapping

In traditional WOA, the initialization of the population is usually random, which may lead to the uneven initial position of the algorithm in the search space and affect the search efficiency. To solve this problem, the improved Tent chaotic mapping algorithm introduced in this paper can generate an initial population that is more evenly distributed in the search space. This uniform initial distribution helps the algorithm to better cover the entire search space from the beginning, thereby improving the global search ability. The formula is as follows:

$$X(t+1)=\begin{cases}2X(t), & X(t)<0.5\\ 2[1-X(t)], & X(t)\geq 0.5\end{cases} \tag{12}$$

(2) Adaptive weight

The adaptive weight method is another innovation point in this paper. It significantly improves the global search ability and convergence speed of the algorithm by dynamically adjusting the exploration and development behavior of individuals in the search process. In this method, the position update of each whale individual is adjusted by a weight that considers the distance between the current solution and the global optimal solution. This weight gradually decreases as the number of iterations increases, thereby balancing the randomness and certainty in the search process. The improved position update formula and ω calculation formula are as follows:

$$X(t+1)=\begin{cases}\omega(t)\cdot X^{*}(t)-A\cdot D & p<0.5\\ D\cdot e^{bl}\cdot\cos(2\pi l)+\omega(t)\cdot X^{*}(t) & p\geq 0.5\end{cases} \tag{13}$$

$$X(t+1)=\omega(t)\cdot X_{r}(t)-A\cdot D \tag{14}$$

$$\omega(t)=0.2\cos[\frac{\pi}{2}(1-\frac{t}{T_{\max}})] \tag{15}$$

where $X(t+1)$ is the position vector of the current solution.

4. The Establishment of Temperature Compensation Model

The selection of parameters in SVR directly impacts its training and generalization capabilities. Three key parameters, namely the penalty factor C, tolerance parameter ε, and kernel parameter σ, must be carefully adjusted. To enhance the temperature compensation effect, the parameters in the SVR model are optimized through improvements to the WOA algorithm. The resulting set of optimal parameters is then utilized for temperature compensation to enhance accuracy. The overall framework of the temperature compensation model, based on the improved WOA-SVR, is illustrated in Fig. 4. The construction concept is detailed as follows:

Step 1: Obtain and preprocess the temperature data, and divide it into a test set and a training set.

Step 2: Determine the training sample data set and normalize it. To speed up the solution and improve the compensation accuracy, this paper also uses the min-max standard method to normalize the data. The formula is:

$$X_{new}=\frac{x-x_{\min}}{x_{\max}-x_{\min}}\ 1 \tag{16}$$

Step 3: Optimize the model parameters. First, initialize the SVR model parameters and optimize the key parameters using an improved WOA algorithm. Set the population number to N and use the Tent chaotic map to initialize the population, obtaining the initial parameters and individual position X. Determine the optimization parameters and range, then calculate to find the individual position with the optimal fitness value. Record the optimal individual and position, and update A and C. Depending on the value of A, adopt different location update strategies and improve the location update with adaptive weight. In the temperature compensation model, the mean square error is typically selected as the fitness function.

Step 4: Determine whether the algorithm satisfies the termination condition. If the algorithm terminates the iteration, it shows that the current value is the optimal parameter combination; if the algorithm continues to calculate, it indicates that the optimal value has not been reached until the termination condition is satisfied. The optimal parameter combination is output and assigned to the SVR model to construct an improved WOA-SVR model, and the prediction accuracy of the model is

verified by the test set.

Step 5: Temperature compensation is performed on the verified model, and the results after compensation are obtained by denormalization.

The flow chart of the above steps is shown in Fig. 4:

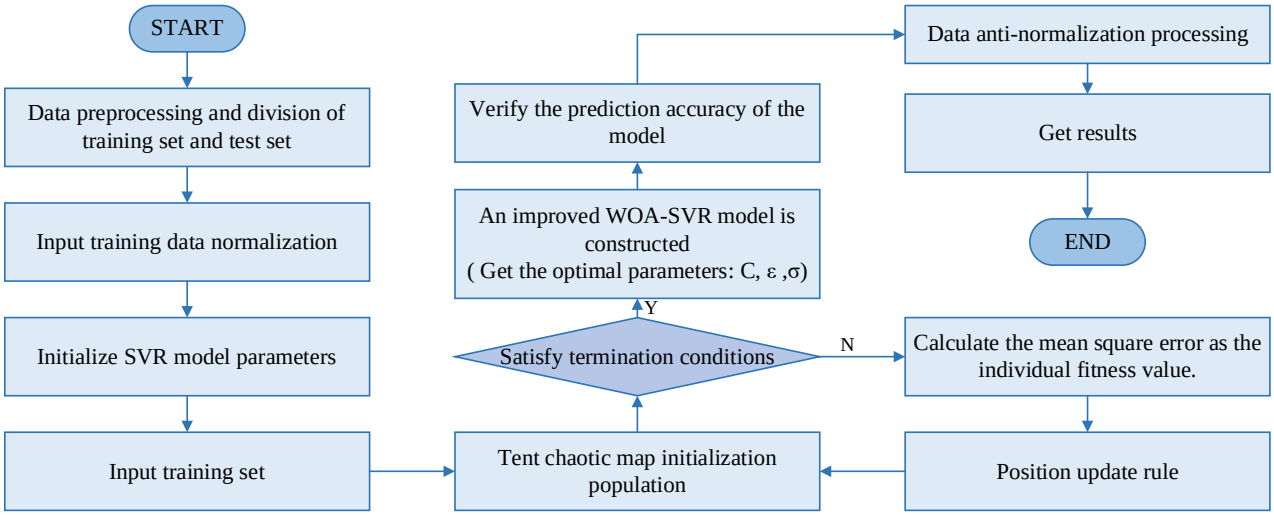

Fig. 4 General flow chart of temperature compensation model

5. Simulation and Experiment

In this paper, MATLAB R2020a simulation software is used to experiment with the operating environment of Windows 11 (64bits). The data set used in the experiment is a sensor open source temperature data set of Github. Some of its temperatures and their corresponding dates and times are shown in the following Table 1:

Table 1 Partial temperature data

Time	Temperature
2022.06.29 13:06:30	38
2022.06.29 13:07:00	38
2022.06.30 11:20:00	23
2022.06.30 11:40:00	23
2022.06.30 12:00:00	23
2022.06.30 12:20:00	24
2022.06.30 12:40:00	25
2022.06.30 13:00:00	25
2022.06.30 13:20:00	25
2022.06.30 13:40:00	26

First, data preprocessing is performed on the above data set to eliminate outliers and null values. Then 80 % of the data set is selected as the training set, and the remaining 20 % is used as the test set. At the same time, in the algorithm design and comparison, the number of iterations set in this paper is 100, the number of populations is 50, and the parameter dimension is 3. Finally, the temperature compensation is carried out according to the steps of Fig. 5, and the following temperature comparison diagram is obtained:

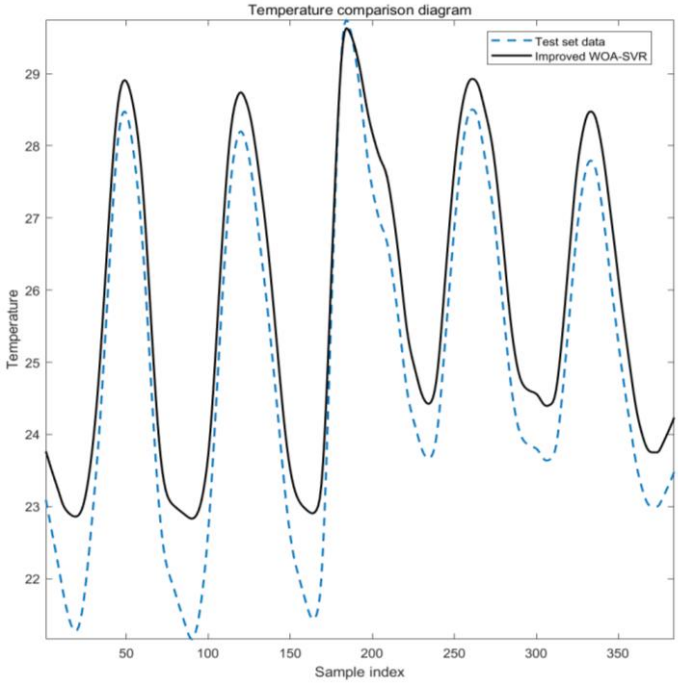

Fig. 5 Temperature comparison diagram

To more intuitively reflect the superiority of the proposed algorithm, this paper will compare it with the particle swarm optimization support vector regression (PSO-SVR) prediction model and the unmodified WOA-SVR prediction model. The comparison between the compensated temperature of each algorithm and the test temperature is integrated as shown in Fig. 6:

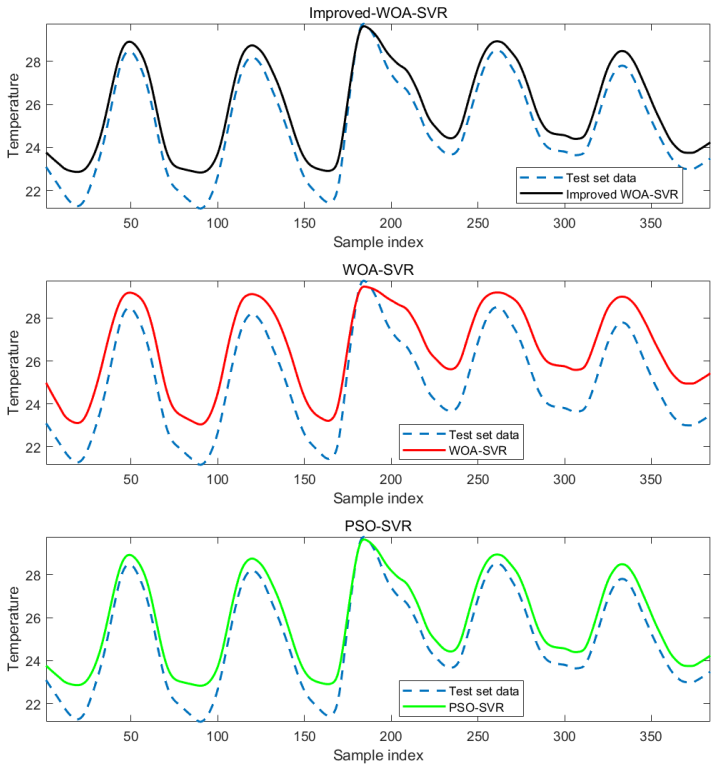

Fig. 6 Algorithm comparison diagram

However, it can be seen from the above diagram that the compensation temperature diagram obtained by PSO-SVR is similar to the compensation temperature diagram obtained by the improved WOA-SVR. To show the superiority of the proposed algorithm more intuitively, four different evaluation indexes are introduced here: mean absolute percentage error (M_{APE}), mean square error (M_{SE}), determination coefficient (R^2), and relative standard deviation (R_{SD}).

In the above formula, y_i and y_i represent the compensated temperature value and the initial temperature value respectively, and $\bar{y}$ represents the average value of the initial temperature value. The closer the M_{APE} and M_{SE} are to 0, the better the model selection and fitting, leading to more successful data prediction and a closer approximation to the perfect model. The greater the value, the greater the error; from the above expression, it can be known that the normal value range of R^2 is [0, 1]. The closer it is to 1, the stronger the explanatory power of the variable of the equation to y is, and the model fits the data well. The R_{SD} value represents the degree of dispersion of the data. The smaller the value, the smaller the degree of dispersion, and the higher the prediction accuracy. On the contrary, the larger the value is, the greater the dispersion is, and the smaller the prediction accuracy is. The results of each model evaluation index are shown in Fig. 7 and Table 2.

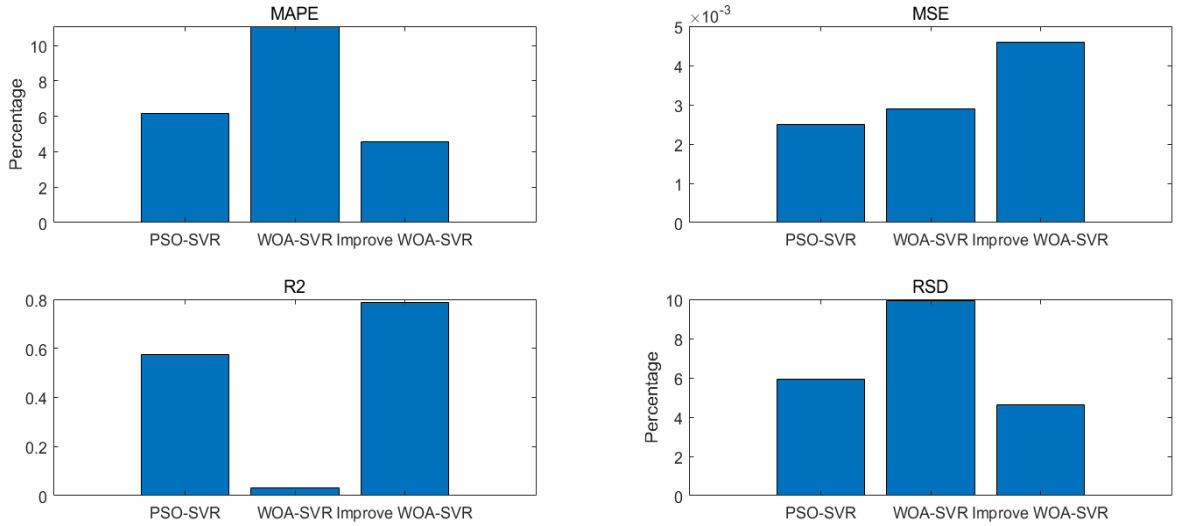

Fig. 7 Evaluation index comparison chart

Table 2 Comparison table of each evaluation index

Model	M_{APE}	M_{SE}	R^2	R_{SD}
PSO-SVR	6.1557%	0.0025	0.5765	5.9408%
WOA-SVR	11.0927%	0.0029	0.0300	9.9327%
Improved WOA-SVR	4.5557%	0.0046	0.7882	4.6412%

It can be seen from the above diagram and table that the M_{APE} value and R_{SD} value of the improved WOA-SVR prediction model are lower than those of the PSO-SVR model and the WOA-SVR model. The value of the correlation coefficient is 0.7882, indicating that the improved WOA-SVR model has better interpretation ability and better goodness of fit. It also shows the superiority of the model's performance and can better perform temperature compensation. As shown in Tab. 2, the range of M_{SE} values of the three methods is 0 ~ 0.0050. Although the M_{SE} value of the method used in this paper is slightly lower than the above two comparison models, the time required (not shown in the table) is far better than the other two models, and the other three aspects are better than the two comparison models, which means that the method used in this paper has a good effect in prediction. The results of comparative analysis and prediction show that the prediction accuracy of the improved WOA-SVR prediction model is higher than that of PSO-SVR and WOA-SVR prediction models.

6. Conclusion

In this paper, an improved WOA-SVR model is proposed to solve the load management requirements in the steel industry by studying the temperature compensation method of monitoring sensors. The simulation results lead to the following conclusions:

(1) By comparing the experimental results, it is found that the improved WOA-SVR model has better performance in temperature compensation, accurately predicts the influence of temperature change on sensor data, and improves the accuracy and stability of the monitoring system.

(2) By improving the accuracy of compensation, this study indirectly reduces the cost required by the steel industry and improves the levels of industrial automation.

(3) This study also promotes the sustainable development of the steel industry and related industries.

(4) The experimental data sets are derived from specific environmental conditions and may not fully represent the actual operating environment in all steel industries.

(5) Although the proposed improved WOA-SVR model shows good performance in experiments, the applicability of the model in different types of sensors and a wider temperature range has not been verified.

In the future, further optimization of the improved WOA-SVR model can enhance its efficiency and accuracy in practical applications. Additionally, exploring the model's applicability in monitoring sensors across various industries could be beneficial. Furthermore, integrating the model with other advanced technologies, such as artificial intelligence, could enhance the monitoring system's performance to meet evolving load management needs.

7. Acknowledgments

This work was supported by the Science and Technology Project of China Southern Power Grid Co., Ltd., under Grants YNKJXM20240002, and the National Key Research & Development Program of China under Grants 2023YFB2407300.

Conflicts of Interest

The authors declare no conflict of interest.

References

[1] Y. D. Wang, D. Wang, and X. P. Shi, “Sustainable Development Pathways of China's Wind Power Industry Under Uncertainties: Perspective from Economic Benefits and Technical Potential,” Energy Policy, vol. 182, article no. 113737, November 2023.

[2] U. K. Vates, B. P. Sharma, N. J. Kanu, E. Gupta, and G. K. Singh, “Modeling and Optimization of IOT Factors to Enhance Agile Manufacturing Strategy-Based Production System Using SCM and RSM,” Smart Science, vol 10, no. 2, pp. 158-173, 2022.

[3] E. Gupta, N. J. Kanu, M. S. Agrawal, A. A. Kamble, A. N. Shaikh, U. K. Vates, et al., “An Insight into Numerical Investigation of Bioreactor for Possible Oxygen Emission on Mars,” Materials Today: Proceedings, vol. 47, no. 14, pp. 4149-4154, 2021.

[4] A. D. Halwe, S. J. Deshmukh, N. J. Kanu, and J. S. Gawande, “Optimization of Combustion Characteristics of Novel Hydrodynamic Cavitation Based Waste Cooking Oil Biodiesel Fueled CI Engine,” SN Applied Sciences, vol. 5, no.2, article no. 65, February 2023.

[5] C. L. Wang, S. D. C. Walsh, Z. H. Weng, M. W. Haynes, D. Summerfield, and A. Feitz, “Green Steel: Synergies between the Australian Iron Ore Industry and the Production of Green Hydrogen,” International Journal of Hydrogen Energy, vol. 48, no. 83, pp. 32277-32293, October 2023.

[6] U. K. Vates, N. J. Kanu, E. Gupta, G. K. Singh, B. P. Sharma, and V. Pandey, “Optimization of Electro Discharge Critical Process Parameters in Tungsten Carbide Drilling Using L9 Taguchi Approach,” Materials Today: Proceedings, vol. 47, no. 11, pp. 3227-3234, 2021.

[7] S. Chavan, N. J. Kanu, S. Shendokar, B. Narkhede, M. K. Sinha, E. Gupta, et al., “An Insight into Nylon 6, 6 Nanofibers Interleaved E-glass Fiber Reinforced Epoxy Composites,” Journal of The Institution of Engineers (India): Series C, vol. 104, no. 1, pp. 15-44, February 2023.

[8] B. K. Gonfa, D. Sinha, U. K. Vates, I. A. Badruddin, M. Hussien, S. Kamangar, et al., “Investigation of Mechanical and

Tribological Behaviors of Aluminum Based Hybrid Metal Matrix Composite and Multi-Objective Optimization," Materials, vol. 15, no. 16, article no. 5607, August 2022.

[9] X. Li, S. C. Ke, Y. Li, W. Jin, X. H. Fu, G. W. Fu, et al., "Temperature Compensation Based on BP Neural Network with Small Sample Data for Chloride Ions Optical Fiber Probe," Optics & Laser Technology, vol. 176, article no. 110973, September 2024.

[10] Y. Wang, X. L. Sun, T. T. Huang, L. Y. Ye, and K. C. Song, "Cold Starting Temperature Drift Modeling and Compensation of Micro-Accelerometer Based on High-Order Fourier Transform," Micromachines, vol. 13, no. 3, article no. 413, March 2022.

[11] W. J. Sheng, H. T. Lou, J. F. Pan, J. X. Wen, and G.D. Peng, "Online Temperature Drift Compensation of Fabry-Perot Filter Based on Machine Learning and Linear Fitting," Sensors and Actuators A: Physical, vol.363, article no. 114774, December 2023.

[12] L. Gan, J. B. Wang, and, Y. T. Zhou, "A Sub-Millinewton Resolution Biaxial Force Sensor with Temperature Self-Compensation for Vascular Intervention," Sensors and Actuators A: Physical, vol. 364, article no. 114833, December 2023.

[13] H. Zhang, W. P. Chen, L. Yin, and Q. Fu, "Design of MEMS Gyroscope Interface ASIC with On-chip Temperature Compensation," Measurement, vol. 220, article no. 113331, October 2023.

[14] S. Tian, M. Xiong, M. Chen, Y. Cheng, S. J. Deng, H. Q. Liu, et al., "Highly Sensitive Cascaded Fiber SPR Sensor With Temperature Compensation," Optics Communications, vol. 233, article no. 129277, April 2023.

[15] S. Zhao, C. F. Guo, C. N. ke, Y. L. Zhou, and X. W. Shu, "Temperature Drift Compensation of Fiber Strapdown Inertial Navigation System Based on GSA-SVR," Measurement, vol. 195, article no. 111117, May 2022.

[16] M. J. Ouyang, J. L. Gao, A. Li, X. G. Zhang, C. Shen, and H. L. Cao, "Micromechanical Gyroscope Temperature Compensation Based on Combined LSTM-SVM-DBN Algorithm," Sensors and Actuators A: Physical, vol. 369, article no.115128, April 2024.

[17] P. Y. Chen, Z. Y. Mao, C. Y. Wang, C. Y. Lu, and J. Q. Li, "A Novel RBFNN-UKF-Based SOC Estimator for Automatic Underwater Vehicles Considering a Temperature Compensation Strategy," Journal of Energy Storage, vol. 72, Part B, article no. 108373, November 2023.

[18] F. X. Yu, C. N. Li, and Y. H. Shao, "DNTC: An Unsupervised Deep Networks for Temperature Compensation in Non-Stationary Data," Engineering Applications of Artificial Intelligence, vol. 127, Part B, article no. 107319, January 2024.

[19] X. L. Zhao, Y. Chen, G. H. Wei, L. L. Pang, and C. X. Xu, "A Comprehensive Compensation Method for Piezoresistive Pressure Sensor Based on Surface Fitting and Improved Grey Wolf Algorithm," Measurement, vol. 207, article no. 112387, February 2023.

[20] L. J. Tian, Y. X. Niu, C. W. Huang, H. Y. Li, Y. Pang, and Y. Q. Yang, "A Novel Temperature-Compensation Method Based on Correlation Analysis for Multi-FOG INS," Chinese Journal of Aeronautics, vol. 36, no. 6, pp. 279-287, June 2023.

[21] S. Liu, H. Z. Yang, Z. Q. Mei, X. Y. Xu, and Q. E. He, "Ultra-Wideband High Accuracy Distance Measurement Based on Hybrid Compensation of Temperature and Distance Error," Measurement, vol. 206, article no. 112276, January 2023.

[22] E. D. Bobobee, S. L. Wang, P. Takyi-Aninakwa, C. Y. Zou, E. Appiah, and N. Hai, "Improved Particle Swarm Optimization–Long Short-Term Memory Model with Temperature Compensation Ability for the Accurate State of Charge Estimation of Lithium-Ion Batteries," Journal of Energy Storage, vol. 84, Part A, article no. 110871, April 2024.